Measurement Science and Technology

PAPER • OPEN ACCESS

# Machine learning method for predicting the influence of scanning parameters on random measurement error

To cite this article: Uroš Urbas *et al* 2021 *Meas. Sci. Technol.* **32** 065201

View the article online for updates and enhancements.

You may also like

- Evaluation of performance of machine learning methods in mining structure–property data of halide perovskite materials
Ruoting Zhao, , Bangyu Xing et al.

- A review on digital mapping of soil carbon in cropland: progress, challenge, and prospect
Haili Huang, Lin Yang, Lei Zhang et al.

- Artificial intelligence for photonics and photonic materials
Davide Piccinotti, Kevin F MacDonald, Simon A Gregory et al.

This content was downloaded from IP address 202.8.112.182 on 19/06/2023 at 12:27

OPEN ACCESS
IOP Publishing
Measurement Science and Technology
Meas. Sci. Technol. 32 (2021) 065201 (8pp) https://doi.org/10.1088/1361-6501/abd57a

# Machine learning method for predicting the influence of scanning parameters on random measurement error

**Uroš Urbas, Daria Vlah and Nikola Vukašinović**

Faculty of Mechanical Engineering, University of Ljubljana, LECAD, 1000 Ljubljana, Slovenia

E-mail: nikola.vukasinovic@lecad.fs.uni-lj.si

Received 22 September 2020, revised 27 November 2020
Accepted for publication 18 December 2020
Published 29 March 2021

**Abstract**
Measurements of technical objects can be done with contact and non-contact approaches. Contact methods are accurate but slow. On the other hand, non-contact methods deliver rapid point acquisition and are increasingly being used as their precision mounts. However, multiple scanning parameters such as the incident angle, object colour and scanning distance influence the measurement error and uncertainty when capturing the geometry of the object. With the aim of creating a generalised model that considers the influence of the aforementioned scanning parameters with satisfactory accuracy, a model for predicting the random measurement error based on machine learning (ML) is proposed in this study. Data acquired from measurements with varying scanning distances, incident angles and surface colours were used to train ML models. The tested ML methods included linear regression, support vector machine, neural network, k-nearest neighbour, AdaBoost and random forest. The best-performing trained model was the random forest, with a standard deviation of relative differences of 1.46% for the case of red surfaces, and 5.2% for the case of an arbitrarily coloured surface, which is comparable to results achieved with model-based methods. The trained models and the data are available online.

Keywords: scanning parameters, machine learning, random measurement error

(Some figures may appear in colour only in the online journal)

## 1. Introduction

The field of optical inspection methods and specifically laser triangulation measurements has developed immensely as it enables fast data acquisition times [1, 2]; however, problems remain concerning the accuracy and the reliability of the measurements [3]. The main advantages over tactile measurements [4] include their contactless measurement and high sampling rate [5–7].

Original content from this work may be used under the terms of the Creative Commons Attribution 4.0 licence. Any further distribution of this work must maintain attribution to the author(s) and the title of the work, journal citation and DOI.

It is important to identify the random measurement error (RME) of scanning results. The RME is a component of the measurement error that in replicate measurements varies in an unpredictable manner [8]. It can also be referred to as the measurement noise. The RME quantifies the scatter (displacement) of the measured point from the expected position and forms a distribution when measuring a set of repeated measurements. It depends on a few factors, the most important of these being the angle of inclination and distance of the sensor from the surface [9]. Other factors also influence the RME, e.g. the colour [10], the texture of the surface [11, 12] and the reflectiveness. A study by Gerbino *et al* [1] pointed out that the object-to-scanner angular position has a statistically significant effect on the measurement accuracy, while both the lighting and the filter factors are not (statistically) significant.

 © 2021 The Author(s). Published by IOP Publishing Ltd Printed in the UK

In a study by Vukašinović *et al* [13] those parameters were gathered into an equation model to predict and evaluate the quality of the measurement results. Reflectivity is, in general, a function of more parameters, like surface roughness and ambient light, but the most important parameter that was observed was the colour of the surface for the matte Lambertian reflection in the research objects [13].

The RME expresses the quality of the measurement. Scanning parameters that provide the least point deviations can be found using the least-squares method as described by Isa *et al* [14]. By exploring the principles of laser triangulation, the colour error can be obtained via the Phong model, whereas the relationship between the measurement error and colour can be achieved through experiments as studied by Li *et al* [15]. Based on the results of their study, a colour error compensation method was proposed, which produces a colour-error library according to the error of the different colours. The experimental results showed that the system would reduce the error to 10% and retain the colour measurement error to within 90 $\mu$m.

Measurement uncertainty can be expressed based on repeated measurements (type A) [16], or using the available information to propagate the uncertainties through the measurement (type B). Type B evaluation can include information from previous measurements, manufacturer's specifications and data attained from the calibration process [8]. When only the random error is included in the estimation of the measurement uncertainty, it expresses the precision of the measurement. The measurement precision can be used to define the measurement repeatability [17]. In a study by Mohammadikaji *et al* [18], the authors developed a mathematical framework for statistical modelling and propagation of the uncertainties in 3D inspection using laser scanners. The authors split the sources of uncertainties into three main groups: laser detection uncertainty, positioning uncertainty and camera intrinsic calibration uncertainty. By evaluating the adeptness of the measurement in several different sensor configurations, they were able to apply the proposed approach (based on analytic methods linearly approximated by Taylor series) to rapid prototyping of demanding laser triangulation setups, where the precision must meet certain tolerances. The standard deviation (SD) of a group of points is a good indicator of a random error in the measurement. A study by Gestel *et al* [5] proves the great influence of scan depth on the SD. A study by Li *et al* [19] presents a scanner posture optimisation method for reducing the measurement uncertainty of laser scanning data for complex surfaces. The method optimises the pitch and deflection angle and finds an optimal scanning posture within the posture adjustment interval so that the measurement uncertainty in the scanning area is minimised. It can effectively reduce the measurement uncertainty represented by the SD by 15%, depending on the complexity of the scanning surface.

Machine learning (ML) methods can likewise be used for determining the RME. Moreover, ML methods are more commonly being used to improve the processes related to non-contact 3D scanning. One of the applications presented in [20] is the simplification of information about geometry achieved from point clouds. The authors tested several clustering methods (tree decomposition, binary partition, k means and hierarchical clustering) to create clusters based on the SD of points in order to recognise which points are on the same surface. With this method, it is possible to find distinct geometrical features of the object from the point cloud. In the paper, a method for feature-sensitive simplification of 3D point clouds that is based on $\varepsilon$-insensitive support vector regression ($\varepsilon$-SVR) is presented.

ML algorithms can also be used for clustering to detect cracks on the scanned surface of steel slabs [21], where the support vector machine (SVM) was used as a classifier. In a study by Tootooni *et al* [22] the researchers used a novel method to invoke a spectral graph of Laplacian eigenvalues as a function derived from the laser-scanned 3D point cloud data in combination with various ML techniques. The result was a new approach that categorised the dimensional variance of an additive manufactured component by sampling less than 5% of the (per part) acquired 2 million 3D point cloud data. Six ML approaches were tested: sparse representation, k-nearest neighbour (kNN), neural network, naïve Bayes, SVM and decision tree. Of these, the highest classification accuracy ($F$-score > 97%) was achieved using the sparse representation technique. In a study by Wissel *et al* [23] artificial neural networks (ANNs) were used for calibration purposes of a galvanometric triangulation device based on two mirrors. Other supervised data-driven methods such as ridge regression, SVR and a Gaussian method were compared with the ANNs. The authors demonstrated that the data-driven models outperformed the model-based methods available (based on ten-fold cross-validation) and delivered comparable efficiency relative to a calibration memorisation lookup table (physical model/manual setup). The findings indicate that generalisation problems can emerge from the off-the-shelf use of ANNs. It has proved beneficial to limit the space of functions using kernel-based learning. ML methods have proven to be beneficial when used for calibration purposes, as they avoid constructing mathematical models, which are tied to specific applications. In comparison, the model-based techniques work with the noise-free data assumption and, therefore, struggle with measurement noise and imperfect data [24], which is also valid for ML methods. Due to the flexibility and the possibility of creating a model without a precise knowledge of the process, the approach of using data-driven techniques is more widespread [25]. However, they present different challenges, which include small or incomplete datasets, high dimensional data, process non-linearities and process delays and dynamics. The authors in [9] proposed a new model for defining the optimal settings of morphological parameters in contactless laser scanning, which was intended to improve the measurement accuracy. The scanning distance and scanning incidence angle were identified as two of the most influencing factors based on surface morphology. A mathematical prediction model for estimating the SD of the final surface was developed in terms of the above scanning parameters using response surface methodology (RSM). To improve the accuracy, the model was further optimiwed using a modified particle swarm optimisation (MPSO) algorithm. The proposed methodology reduced the SD by 21.6% and 11.77%, respectively. The model was created and tested only on white surfaces. The developed MPSO algorithm shows significant improvement over PSO results as well as the RSM method by 6.7% and 27.6%, respectively. The mean absolute percentage error was used as a metric to evaluate the performance of the model. The higher value of the determination coefficient ($R^2 = 98.02\%$) indicated that less than 1.98% of the total variations in SD are not clarified by the model. If a model is created that returns the measurement error depending on the measurement conditions, that can be used for path planning for 3D scanning devices [26].

Our study aims to use ML methods for predicting the RME given the scanning parameters. The intent is to develop a more accurate model for determining the RME than was developed in the study by Vukašinovič *et al* [13]. The usefulness of the approach has previously been proven in a study by Korošec *et al* [27], where a methodology developed on a flat surface was further used on a curved surface to reduce the random error by changing the measurement parameters. ML methods can be used for classification or regression tasks, depending on the output variable. In this case, the RME is a numerical value and the attributes are all numerical; therefore, regression methods will be used. This presents a novel approach for creating a data-driven model using ML, capable of determining RME by considering the scanner position and surface properties.

### *1.1. Data acquisition*

The measurement data of the study [13] were the basis for creating several prediction models of the RME. The prediction models were built with ML methods and their results were later compared with measured values.

The data were acquired with a system based on the principle of laser optical triangulation. The measurement system was a Zephyr KZ-50 laser triangulation measuring sensor from Kreon mounted on a numerically controlled machine. The measurements were done in a controlled environment with constant temperature, humidity and dimmed lights with no direct light impact on the measurement surface or the sensor. The system is described in detail in article [13].

The RME is a value that presents information about the expected spread of the measured points from the ideal position, and is usually presented as an SD of the displacements of measured points from a reference surface. In this study, this is a scatter of the measured point cloud from the ideal surface.

According to Gestel *et al* [5], the SD of the residual distances of the measurement points to the plane is a good indication of the random error.

The measurements were carried out on three differently coloured flat stone gauges. The surfaces typically reflect a wider spectrum of light and do not have narrow, monochromatic properties of reflection. A narrow-band filter was used for the sensor and the laser-light intensity and exposure time of the sensor is set according to each surface to obtain a CCD sensor light intensity that is as close as possible for all the samples. The area of interest in the analysis was the reflectance level around the wavelength of 675 nm.

Surfaces of different colours were found to have different reflectivities of that laser wavelength. Red surface reflectivity is 87%, blue 7% and green 23% compared to the white surface. This value shows the intensity of the reflected light from a surface with diffuse matte reflection, compared with the intensity of the light that is reflected from a white surface with Lambertian diffuse reflection [13]. Roughness also plays a role in the reflectivity of the surface. The measured roughness Ra of the red, green and blue stone gauges was 3.34, 3.14 and 1.08 $\mu$m, respectively. The roughness of the surfaces was in the same size range, and should not cause an additional source of error.

### *1.2. Data structure*

The RME was evaluated as an SD of the point cloud scatter. The SD was calculated using the distances of the individual points in a perpendicular direction to the virtual ideally flat surface, which was aligned to the point cloud with the least-squares method. Therefore, the RME was determined with equation (1) for the standard deviation $\sigma$ of the population:

$$\sigma = \sqrt{\frac{\sum_{i=1}^{N} (x_i - \bar{x})^2}{N-1}} \tag{1}$$

where $x_i$ is the individual distance of the point to the flat surface and $\bar{x}$ is the average of the distances of the $N$ number of points in a measurement.

Seven different measurement distances ranging from 130 mm to 190 mm, and 14 different measurement angles ranging from 0° to 65° with a 5° increment were made. Therefore, each surface was measured with 98 different combinations of measuring distance and incident angle. The combinations were tested in a random order to minimise any possible systematic error.

The RME for the individual surfaces is illustrated in figure 1 for the red, figure 2 for the green, and figure 3 for the blue surface. The figures display how the RME is dependent on the angle of inclination and the distance of scanning, while also considering the reflectivity of the surfaces. From these figures, it is already possible to determine the area where the minimum RME would occur. For the red surface, this would be at an angle of inclination of 50°–55° and a distance of 130–140 mm.

The number of acquired points during the scanning procedure is also an indicator of the quality of the measurement [28]. The red surface had the best results and its data were firstly used in the ML process. For a further model that can predict the RME also taking into account the surface colour, the datasets for the green and blue surface were first trimmed so that they only included measurements where the point cloud had at least 1000 points and could therefore represent a trustworthy measurement. The minimum amount of 1000 points was also selected as this is the estimated minimum amount of needed points for reliable surface reconstruction from the point cloud. After the trimming process, the red surface was left with all of the 98

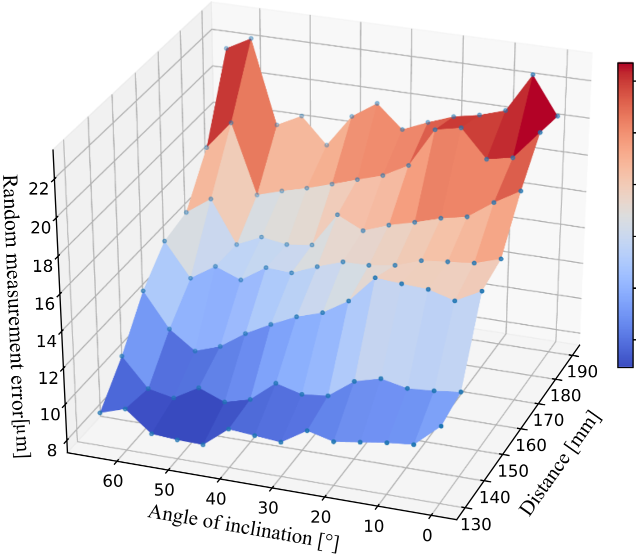


**Figure 1.** Random measurement error on the red surface.

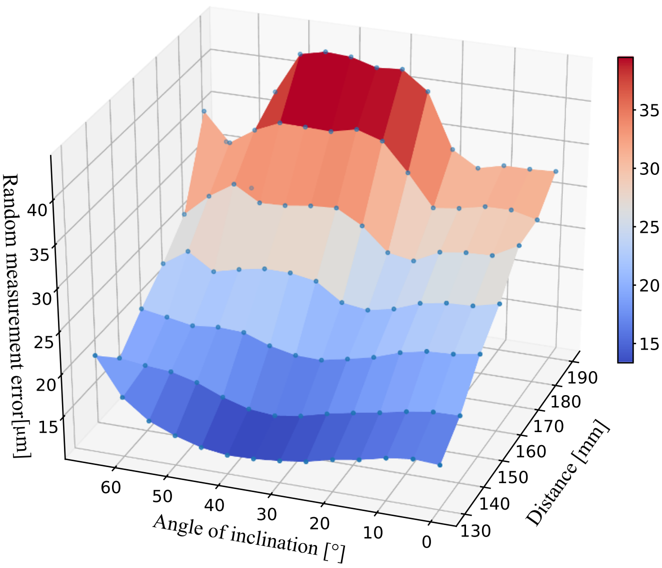


**Figure 2.** Random measurement error on the green surface.

measurements, the green surface with 87, and the blue with 60. These data were used in the ML process. Therefore, the attributes in the data were the scanning distance, scanning incident angle and surface reflectivity rate. The target variable is the RME. The attributes and the target variable all have numerical values.

### *1.3. Research goals*

From figures 1–3 it is possible to see where the best scanning conditions are for each of the surface colours. The red surface also has the smallest RME. However, the goal of the study is to create a model that is able to predict the RME for a given random set of input data for the red colour, and then for all the colours combined. This was previously done in the article [13] with the ANOVA method, which shows the factorial response.

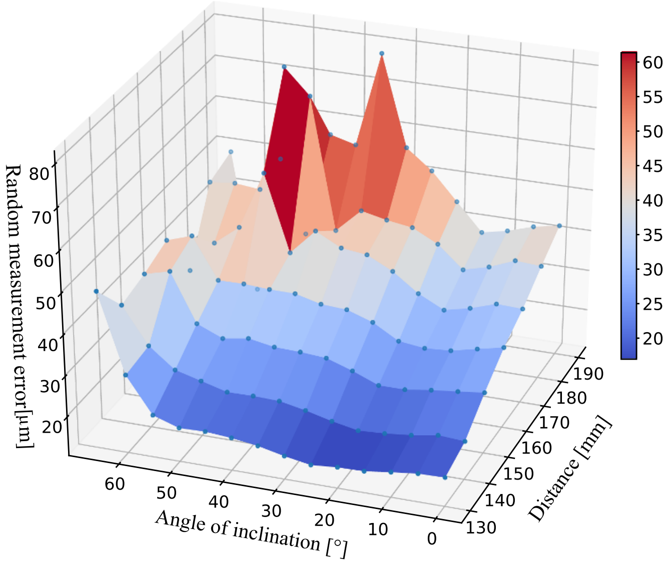


**Figure 3.** Random measurement error on the blue surface.

However, this study aims to create a more accurate model with the use of ML methods.

## 2. Methodology

The used ML methods were linear regression, SVM, ANN, kNN, AdaBoost and random forest.

The parameters, when training on the red surface data, were set to the values described below.

Linear regression, which learns a linear function from the input data and can identify the relationship between the input and output variable, used no regularisation.

SVM was used next, which is an ML technique that performs linear regression in a high-dimension feature space. Its estimation accuracy depends on the proper setting of the parameters [29]. The regression cost in the SVM was set to 0.9 and the complexity bound to 0.15. A radial basis function (RBF) kernel was used.

The ANN is a multi-layer perceptron algorithm that is capable of learning non-linear models. The ANN was set up to use 130 neurons in the hidden layers, a logistic sigmoid activation function and an L-BFGS-B solver for weight optimisation. The maximal number of iterations was set to 150.

The setting for the kNN algorithm, which searches for the closest training examples in the feature space and uses their average as prediction, were set to four neighbours. It used the Euclidean (straight-line) distance, and weights were set according to the distance, which gives closer neighbours of a query point a greater influence than the neighbours further away.

The random forest algorithm creates and uses a collection of decision trees. Each of the trees is constructed from a certain subset of random attributes, from which the best attribute for the split is calculated. The final model performance is based on the majority vote of the developed trees. The number of

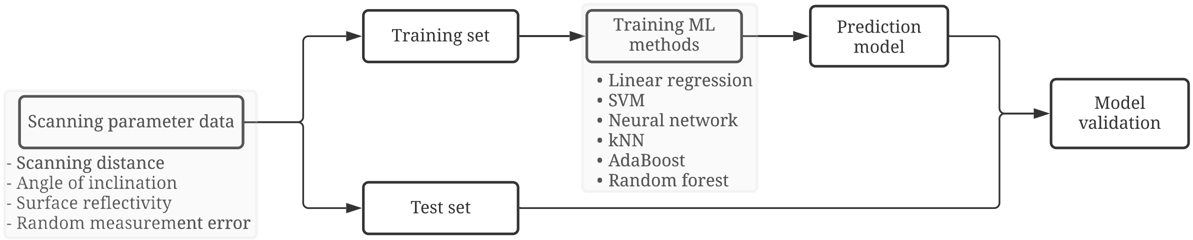


**Figure 4.** Workflow of training, validating and using the models in the study.

**Table 1.** Results of the evaluation for the red-coloured surface.

| Distance (mm) | Angle (°) | Actual value ($\mu$m) | ANOVA prediction ($\mu$m) | Random forest ($\mu$m) | kNN ($\mu$m) |
|---|---|---|---|---|---|
| 160 | 5 | 16.01 | 16.84 | 16.46 | 16.32 |
| 170 | 15 | 16.74 | 17.56 | 16.64 | 16.73 |
| 140 | 30 | 10.43 | 11.25 | 10.33 | 10.60 |
| 160 | 40 | 13.96 | 13.27 | 14.20 | 13.96 |
| 130 | 55 | 8.46 | 8.38 | 8.62 | 8.89 |
| Standard deviation of relative differences (%) | | | 4.7 | 1.46 | 1.86 |

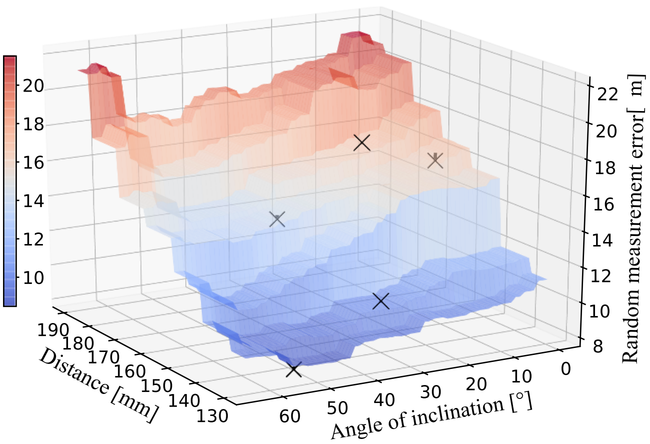


**Figure 5.** Trained random forest model results on the red surface with test data from table 1. The surface represents the prediction model, while the crosses represent the results of the measurement.

**Table 2.** Results of the $N$-fold cross-validation including the reflectivity.

| Model | MSE | RMSE | MAE | $R^2$ |
|---|---|---|---|---|
| kNN | 2.013 | 1.419 | 0.962 | 0.973 |
| Random forest | 2.194 | 1.481 | 0.976 | 0.971 |
| Neural network | 2.365 | 1.538 | 1.086 | 0.969 |
| AdaBoost | 2.621 | 1.619 | 1.165 | 0.965 |
| Linear regression | 11.583 | 3.403 | 2.732 | 0.847 |
| SVM | 21.094 | 4.593 | 3.890 | 0.721 |

trees in the random forest was set to 65 and two attributes were considered at each split.

The AdaBoost model also used 65 estimators (randomly generated trees) with a square regression loss function. The AdaBoost algorithm is an ensemble method. It uses other algorithms and boosts their performance. It uses decision trees with only one node and two leaves. The previous decision tree influences how the next one is constructed. The algorithm focuses on the instances with higher errors with increasing their weights. Moreover, the final result is determined by weighting the results from the individual trees.

Some of the data were excluded from the learning process and used for validating the model. The ML parameters for the algorithms were firstly set to achieve the best result during cross-validation according to the evaluation criteria. The cross-validation splits the training data into a determined number of folds; in this case ten. Each of the folds is then excluded from the learning process and used for testing. This is repeated for all the folds and the result is the average value achieved from all the folds.

The workflow of how the methods were trained and evaluated is presented in figure 4.

To train the methods to determine the RME taking into account the surface colour, ten new measurements on a white surface were also included. Thirteen data instances were excluded from the training set to be used for testing and validation: three for the blue, four for the green and red, and two for the white surface. The white surface has a reflectivity of 100%. The ML methods used were the same as for training on the red-coloured surfaces. No regularisation was used for the linear regression method. The SVM used the RBF kernel, a regression cost of $\varepsilon = 0.95$ and a complexity bound of $C = 0.15$. The neural network used 100 neurons in the hidden layers, an identity activation function and an L-BFGS-B solver. The maximal number of iterations was set to 50. The kNN used four neighbours, Euclidean distance and distance weighting. AdaBoost used 50 trees with a square regression loss function and a learning rate of 0.995. Likewise, the random forest used 50 trees and it used two attributes at each split.

**Table 3.** Results for predictions with the trained random forest model.

| Distance (mm) | Angle (°) | Surface reflectivity (%) | Actual value ($\mu$m) | Random forest ($\mu$m) | Relative deviation (%) |
|---|---|---|---|---|---|
| 160 | 25 | 7 | 31.40 | 28.90 | −7.94 |
| 170 | 15 | 7 | 30.47 | 32.38 | 6.26 |
| 140 | 0 | 7 | 19.79 | 20.19 | 2.01 |
| 160 | 55 | 23 | 23.77 | 25.00 | 5.19 |
| 150 | 30 | 23 | 18.48 | 19.11 | 3.40 |
| 160 | 15 | 23 | 23.79 | 23.83 | 0.17 |
| 130 | 10 | 23 | 15.01 | 15.54 | 3.54 |
| 190 | 0 | 87 | 20.43 | 20.95 | 2.53 |
| 160 | 10 | 87 | 15.87 | 15.91 | 0.27 |
| 150 | 60 | 87 | 11.29 | 11.25 | −0.35 |
| 130 | 10 | 87 | 10.15 | 10.53 | 3.71 |
| 137 | 47 | 100 | 24.30 | 21.75 | −10.48 |
| 188 | 51 | 100 | 22.80 | 20.98 | −7.98 |
| Standard deviation of relative differences (%) | | | | | 5.2 |

The performances of the presented methods are dependent on the choice of $\varepsilon$-SVR parameters ($\varepsilon$, $C$ and kernel). $C$ and $\varepsilon$ have a high influence on the reduction, and higher values of $\varepsilon$ and $C$ will lead to a higher reduction ratio [20].

### *2.1. Criteria for evaluating the results*

The performance estimators used were the mean square error (MSE), root mean square error (RMSE), mean absolute error (MAE) and the correlation coefficient ($R^2$). These parameters are regularly used for assessing the feasibility of the models used in numerical prediction. They all have a positive value. The mean square error gives a higher weight to predictions that have a higher absolute error.

## 3. Results and discussion

The results from the red-coloured surface are presented in table 1. The two best-performing ML methods were kNN and random forest. These two methods are compared in detail with the results acquired with the derived equation from the study [13]. Both of the ML methods had an $R^2 = 0.994$.

According to the SD of the relative differences, the trained random forest model is capable of predicting the RME with an SD of 1.46% and performed best. Its predictions were far more accurate than the predictions with the equation derived from article [13], which was also outperformed by the second-best model, kNN. Figure 5 displays the predictions of the trained random forest model for increments of one degree and a distance of one millimetre. The crosses represent the true measured values, also presented in table 1. The darker crosses represent the data which have higher RME values than the model predicts while the lighter crosses have a lower than predicted value. The lines near the crosses present the difference to the predicted value.

The next training was done on data from multiple surfaces. The training of the models and the $N$-fold cross-validation for all the surface colours showed that the kNN and the random forest models performed best and achieved the highest $R^2$. They also achieved a small MSE, which disproportionately punishes the outlying data, and that indicates that all the data are predicted near the true values. The results are shown in table 2.

The trained models were then used to predict the values for the 13 instances that were excluded from the training process. The random forest model performed best and achieved an MSE of 1.724 ($\mu$m) and a correlation coefficient of 0.956. In this case, it performed far better than the other trained models. Table 3 presents the results for the prediction with the trained random forest model.

The trained model is capable of predicting the RME with an overall SD of 5.2%. The prediction performs worse at a surface reflectivity of 7%, which represents the blue colour, as there were fewer training data available due to the pruning and pre-processing of the data. It had the worst performance at the surface reflectivity of 100%, as there were only eight training data for that value. However, it achieved satisfactory values in the surface reflectivity range of 87%–23%.

## 4. Conclusion and outlook

In the paper, a previously developed method was improved with the principles of ML. The method is able to determine the RME more accurately in relation to the measurement distance, incident angle and surface reflectivity, in comparison to the previously developed method. This presents a novel approach for creating a data-driven model for predicting the RME of laser triangulation scanners using ML. The model is capable of determining the RME in the environmental conditions that were used during the study. To be generally useful in all conditions, parameters such as lighting should be included in the training of the model. However, it was indicated in the study how this could be achieved.

The procedure of determining the RME in the study is straightforward and can be easily implemented for other types of laser triangulation scanners.

Multiple ML methods were tested for each case and the random forest gave the best results for both instances.

The performance of all the methods depends greatly on the setting of the parameters. Moreover, testing multiple methods can cause overfitting of the model to the data, as the best performing model is possibly only best on the selected data. If there were more training data available it is plausible that other methods would perform better, as, for instance, neural networks perform better with bigger databases.

Given that the models predict the quality of the measurements, they can be used for optimally setting the scanning parameters in an automated setting. This can easily be achieved by calculating the normal of the surface and setting the camera to consider the model's output.

More measurement instances with varying surface colours should be included in the training process in further work, to increase the accuracy of the model.

## Data availability statement

The trained models and training and test data are available on Zenodo under open access, where they can be downloaded: https://doi.org/10.5281/zenodo.4009138.

## Acknowledgments

The research was partly financed by the Slovenian Research Agency (MR No. 51899).

## Disclaimer

Any mention of commercial products is for information only; it does not imply endorsement by the authors.

## ORCID iD

Uroš Urbas https://orcid.org/0000-0002-5749-5396

## References

[1] Gerbino S, Del Giudice D M, Staiano G, Lanzotti A and Martorelli M 2016 On the influence of scanning factors on the laser scanner-based 3D inspection process *Int. J. Adv. Manuf. Technol.* **84** 1787–99
[2] Novak-Marcincin J, Torok J, Novakova-Marcincinova L, Barna J and Janak M 2014 Use of alternative scanning devices for creation of 3D models of machine parts *Teh. Vjesn.* **21** 177–81
[3] Chao B, Yong L, Jian-guo F, Xia G, Lai-peng L and Pu D 2015 Calibration of laser beam direction for optical coordinate measuring system *Measurement* **73** 191–9
[4] Stein M, Wedmann A, Jantzen S, Hierse K and Kniel K 2020 Involute gear calibration using tactile CMMs in scanning mode *Meas. Sci. Technol.* **31** 075003
[5] Van Gestel N, Cuypers S, Bleys P and Kruth J-P 2009 A performance evaluation test for laser line scanners on CMMs *Opt. Lasers Eng.* **47** 336–42
[6] Urbas U, Zorko D and Vukašinović N 2020 Model-based geometric inspection of polymer spur gears *Proc. TMCE 2020 Tools Methods Compet. Eng. Thirteen. Int. Tools Methods Compet. Eng. Symp. TCME 2020* vol 81 pp 331–42
[7] Urbas U, Zorko D, Černe B, Tavčar J and Vukašinović N 2021 A method for enhanced polymer spur gear inspection based on 3D optical metrology *Measurement* **169** 108584
[8] Joint Committee for Guides in Metrology (JCGM 106:2012) 2012 Evaluation of measurement data—the role of measurement uncertainty in conformity assessment
[9] Pathak V K and Singh A K 2017 Optimization of morphological process parameters in contactless laser scanning system using modified particle swarm algorithm *Measurement* **109** 27–35
[10] Vukašinović N, Bračun D, Možina J and Duhovnik J 2010 The influence of incident angle, object colour and distance on CNC laser scanning *Int. J. Adv. Manuf. Technol.* **50** 265–74
[11] Vukašinović N, Korošec M and Duhovnik J 2010 The influence of surface topology on the accuracy of laser triangulation scanning results *Stroj. Vestn. J. Mech. Eng.* **56** 23–30
[12] Mueller T, Poesch A and Reithmeier E 2015 Measurement uncertainty of microscopic laser triangulation on technical surfaces *Microsc. Microanal.* **21** 1443–54
[13] Vukašinović N, Bračun D, Možina J and Duhovnik J 2012 A new method for defining the measurement-uncertainty model of CNC laser-triangulation scanner *Int. J. Adv. Manuf. Technol.* **58** 1097–104
[14] Isa M A and Lazoglu I 2017 Design and analysis of a 3D laser scanner *Measurement* **111** 122–33
[15] Li S, Jia X, Chen M and Yang Y 2018 Error analysis and correction for color in laser triangulation measurement *Optik* **168** 165–73
[16] Joint Committee for Guides in Metrology (JCGM 100:2008) 2008 Evaluation of measurement data—guide to the expression of uncertainty in measurement
[17] Joint Committee for Guides in Metrology (JCGM 200:2012) 2012 International vocabulary of metrology—basic and general concepts and associated terms (VIM)—3rd edn
[18] Mohammadikaji M, Bergmann S, Irgenfried S, Beyerer J, Dachsbacher C and Wörn H 2016 A framework for uncertainty propagation in 3D shape measurement using laser triangulation *2016 IEEE Int. Instrum. Meas. Technol. Conf. Proc.* pp 1–6
[19] Li Q, Huang X and Li S 2019 A laser scanning posture optimization method to reduce the measurement uncertainty of large complex surface parts *Meas. Sci. Technol.* **30** 105203
[20] Markovic V, Jakovljevic Z and Miljkovic Z 2019 Feature sensitive three-dimensional point cloud simplification using support vector regression *Teh. Vjesn.* **26** 985–94
[21] Veitch-Michaelis J, Tao Y, Walton D, Muller J-P, Crutchley B, Storey J, Paterson C and Chown A 2016 Crack detection in 'as-cast' steel using laser triangulation and machine learning *2016 13th Conf. Comput. Robot Vis. CRV* pp 342–9
[22] Samie Tootooni M, Dsouza A, Donovan R, Rao P K, Kong Z J and Borgesen P 2017 Classifying the dimensional variation in additive manufactured parts from laser-scanned three-dimensional point cloud data using machine learning approaches *J. Manuf. Sci. Eng.* **139** 091005
[23] Wissel T, Wagner B, Stüber P, Schweikard A and Ernst F 2015 Data-driven learning for calibrating galvanometric laser scanners *IEEE Sens. J.* **15** 5709–17

[24] Bos A, Bos M and van der Linden W E 1993 Artificial neural networks as a multivariate calibration tool: modeling the Fe–Cr–Ni system in x-ray fluorescence spectroscopy *Theor. Chim. Acta* **277** 289–95
[25] Vallejo M, de la Espriella C, Gómez-Santamaría J, Ramírez-Barrera A F and Delgado-Trejos E 2019 Soft metrology based on machine learning: a review *Meas. Sci. Technol.* **31** 032001
[26] Ding L, Dai S and Mu. P 2016 CAD-based path planning for 3D laser scanning of complex surface *Proc. Comput. Sci.* **92** 526–35
[27] Korosec M, Duhovnik J and Vukasinovic N 2010 Identification and optimization of key process parameters in noncontact laser scanning for reverse engineering *Comput.-Aided Des.* **42** 744–8
[28] Vukašinović N, Možina J and Duhovnik J 2012 Correlation between incident angle, measurement distance, object colour and the number of acquired points at CNC laser scanning *Stroj. Vestn. J. Mech. Eng.* **58** 23–28
[29] Orange Data Mining—Data Mining (available at: https://orange.biolab.si/) (Accessed 18 February 2020)